Palaeogeography, Palaeoclimatology, Palaeoecology 601 (2022) 111127

Contents lists available at ScienceDirect

Palaeogeography, Palaeoclimatology, Palaeoecology

journal homepage: www.elsevier.com/locate/palaeo

Influence of salinity on glycerol dialkyl glycerol tetraether-based indicators in Tibetan Plateau lakes: Implications for paleotemperature and paleosalinity reconstructions

Qiangqiang Kou [a,b], Liping Zhu [a,b,*], Jianting Ju [a], Junbo Wang [a], Teng Xu [c], Cunlin Li [a,b], Qingfeng Ma [a]

[a] State Key Laboratory of Tibetan Plateau Earth System, Resources and Environment (TPESRE), Institute of Tibetan Plateau Research, Chinese Academy of Sciences, Beijing 100101, China
[b] University of Chinese Academy of Sciences, Beijing 100049, China
[c] Yellow River Institute of Eco-Environmental Research, YRBEEA, Zhengzhou 450004, China

ARTICLE INFO

Keywords:
GDGTs
Lacustrine sediments
Salinity
Tibetan Plateau
Biomarkers

ABSTRACT

Glycerol dialkyl glycerol tetraethers (GDGTs) are powerful molecular tools that are suitable for paleoenvironmental reconstruction. The widely distributed lakes on the Tibetan Plateau (TP) are important terrestrial paleoenvironmental archives. However, studies on the distributions and environmental responses of branched GDGTs (brGDGTs; analyzed by a new method) are scarce, which makes their environmental response uncertain, further hindering the development of paleoclimate research and the reliability of reconstruction results for the TP region. Herein, we report the distribution of brGDGTs and archaeols in surface sediments from 83 lakes and 22 surrounding soils across the TP. The potential source, environmental response of sedimentary brGDGTs, and the implications for the application of GDGT-based indicators are further discussed. Our results indicate that the sedimentary brGDGTs in the TP lakes were mainly produced in-situ. Lake salinity had a noticeable effect on the brGDGT-based temperature indicators. Coupled with the global lake dataset, we found that the methylation index of 5-methyl brGDGTs (MBT'$_{5ME}$) responded to temperature in freshwater lakes, while that of 6-methyl brGDGTs (MBT'$_{6ME}$) showed a better correlation with temperature in saline lakes. However, both indices showed a poor correlation in brackish lakes. These varied responses implied that biological communities producing 5- and 6-methyl brGDGTs were likely to be different, and that 6-methyl brGDGTs might be predominantly synthesized in high-salinity environments. Furthermore, these responses will affect the reliability of paleotemperature records reconstructed by MBT'$_{5ME}$ or MBT'$_{6ME}$ paleothermometers. Therefore, it is essential to evaluate the applicability of these two proxies before using them for paleotemperature reconstruction. In addition, the applicability of GDGT-based salinity indicators on the TP was assessed. Both the archaeol and caldarchaeol ecometric (ACE) and its alternative approach ACE' showed good correlation with lake salinity on the TP, and their high response thresholds to salinity were also noted. It is therefore that these salinity proxies may only be applicable to large paleo-hydrological/salinity fluctuations. In contrast, the isomer ratio of 6- and 7-methyl brGDGTs (IR_{6+7ME} and its revised form IR'_{6+7ME}) was sensitive to salinity and covered different salinity ranges, which may represent novel salinity proxies. The integration of ACE and IR'_{6+7ME} indicators could provide a basis for producing relatively reliable records of paleosalinity and palaeohydrological fluctuations. In conclusion, our work highlights the influence of salinity on GDGT-based indicators and can serve as a reference for paleotemperature and paleosalinity reconstructions in lakes.

* Corresponding author at: State Key Laboratory of Tibetan Plateau Earth System, Resources and Environment (TPESRE), Institute of Tibetan Plateau Research, Chinese Academy of Sciences, Beijing 100101, China.
E-mail address: lpzhu@itpcas.ac.cn (L. Zhu).

https://doi.org/10.1016/j.palaeo.2022.111127
Received 15 March 2022; Received in revised form 14 June 2022; Accepted 18 June 2022
Available online 23 June 2022

1. Introduction

As the center of East Asia, the Tibetan Plateau (TP) plays a vital role in the Asian monsoon and the Northern Hemisphere climate system, and therefore, has always been relevant in climate change research (An et al., 2001; Wu et al., 2012). Widely distributed lakes are good paleoclimate research carriers, and their sediments are important terrestrial climate archives (Castañeda and Schouten, 2011). Lake water salinity, especially in closed lakes in arid and semi-arid areas, depends on the balance among rainfall, runoff, and evaporation (Smol and Cumming, 2000). In addition, lakes provide valuable information about overall moisture and hydrological conditions, which are important for deciphering terrestrial paleoclimates and paleoenvironmental changes (He et al., 2020; Verschuren et al., 2000). A series of salinity proxies have been developed—ostracods and their elemental ratios (Zhang et al., 2004), diatom assemblages (Gasse, 2002; Smol and Cumming, 2000), chironomids (Chen et al., 2009; Heinrichs and Walker, 2006), and carbonate minerals (Muller et al., 1972; Warren, 2010). However, the chemical mineral composition of lakes is easily affected by the environmental conditions after deposition (Ju et al., 2010), which results in the loss of the salinity signal. It is difficult to obtain a continuous paleosalinity record using biological proxies due to their relatively narrow salinity tolerance range and harsh storage conditions (He et al., 2020). With the improvement in liquid chromatography analysis methods, powerful molecular tools suitable for salinity reconstruction have been proposed.

Glycerol dialkyl glycerol tetraethers (GDGTs), lipid biomarkers, have been widely applied in paleoenvironment reconstruction owing to their ubiquity, sensitivity to ambient environment, and resistance to biodegradation (Schouten et al., 2013). GDGTs contain two classes of compounds: isoprenoid GDGTs (iGDGTs) and branched GDGTs (brGDGTs). iGDGTs containing 0–4 cyclopentane moieties (GDGT-0, −1, −2, −3, and crenarchaeol, as well as its regioisomer) can be synthesized by a wide range of archaea (Pearson and Ingalls, 2013; Schouten et al., 2013). Archaeol, a diether of sn-1-glycerol in which C-2 and C-3 are bound to phytanyl residues, is commonly found in Euryarchaeota (Gambacorta et al., 1995). Its dimer, caldarchaeol (GDGT-0), can be synthesized by Crenarchaeota, Nitrososphaeria (synonym "Thaumarchaeota"), and some species of Euryarchaeota (Schouten et al., 2013), and these archaea can survive over a broad salinity range (Turich and Freeman, 2011). In contrast, halophilic Euryarchaeota commonly dominant in hypersaline settings (Jiang et al., 2006; Pancost et al., 2011). Therefore, the archaeol and caldarchaeol ecometric (ACE) index was proposed to estimate the relative contribution of halophilic Euryarchaeota to total Archaea ether lipids, which indicate salinity variation (Turich and Freeman, 2011). This has been developed in subsequent studies and successfully applied to interpret the paleoenvironment (Feakins et al., 2019; Wang et al., 2015). However, studies on high-mountain Tibetan saline lakes (Günther et al., 2014; Li et al., 2016), saline ponds in Inner Mongolia (Li et al., 2019), and tropical ponds (Huguet et al., 2015) have shown that the relationship between the ACE index and salinity is complex. A recent study also found substantial deviations in ACE values in low-salinity lakes in mid-latitude Asia (He et al., 2020). Therefore, it is critical to further investigate lakes in various environmental settings to evaluate the applicability of the ACE index as a proxy for salinity.

BrGDGTs are produced by unknown heterotrophic bacteria (Weijers et al., 2010). The most common molecular structures are distinguished by the number (4–6) and position (α/ω-5 or α/ω-6) of methyl groups, as well as the number (0–2) of cyclopentane rings (De Jonge et al., 2013; Schouten et al., 2013). Previous studies have listed brGDGTs as biomarkers of soils and peats (Sinninghe Damsté et al., 2000); however, in subsequent studies, brGDGTs produced in-situ have also been found in various aquatic environments (De Jonge et al., 2014b; Tierney and Russell, 2009; Tierney et al., 2012; Weber et al., 2015; Xiao et al., 2016). The distribution of brGDGTs was closely related to the ambient environment, and a series of environmental proxies were proposed accordingly. Temperature and pH were initially found to impact brGDGT distribution, which can be indicated by the methylation index of branched tetraethers (MBT) and cyclization index of branched tetraethers (CBT) (Weijers et al., 2007). Recently, a new set of brGDGT isomers (i.e., 5-methyl, 6-methyl, and 5/6-methyl) was identified using the new analytical methods (De Jonge et al., 2014a; Weber et al., 2015) and has been found to respond differently to environmental factors (Dang et al., 2018; Russell et al., 2018). Meanwhile, 7-methyl and unknown brGDGT isomers that elute after 6-methyl brGDGTs have been reported (Ding et al., 2016; Becker et al., 2013), and their degree of isomerization (IR index) may be controlled by the salinity in lacustrine settings (Wang et al., 2021). In addition, other environmental factors, such as oxygen (Martínez-Sosa and Tierney, 2019; Pei et al., 2021; Wu et al., 2021), redox conditions of lakes (Weber et al., 2018; Yao et al., 2020), and soil moisture (Dang et al., 2016), have been shown to affect the distribution of brGDGTs. Initially, this environmental response mechanism considered that the brGDGTs precursor microbes could adapt to various conditions by regulating the composition of their membrane lipids (Pei et al., 2019; Siliakus et al., 2017). However, recent studies have proposed that potential changes associated with microbial communities, rather than the specific mechanism of their membranes adapting to the conditions, influence the distribution of brGDGTs (De Jonge et al., 2019; Weber et al., 2018). Hence, the impact of microbial community composition on the brGDGTs distribution and the degree of environment-dependent influence remain unclear.

In summary, both iGDGTs and brGDGTs are powerful molecular tools as environmental proxies; however, their applicability is strongly dependent on the investigation of modern lake systems. Furthermore, the TP is one of the most densely distributed areas of lakes in the world, and the study of GDGTs on modern lake systems (analyzed by new methods) is extremely scarce, which hinders the development of paleoclimate research and the reliability of reconstruction results in this area. In this study, we investigated the distribution of brGDGTs and archaeol in surface sediments collected from 83 lakes and 22 surrounding soils on the TP (Fig. 1). The selected sampling sites cover a wide range of water depths and areas and vary widely in terms of salinity, temperatures, dissolved oxygen (DO) concentration, pH values, chlorophyll-a concentrations, and fluorescent dissolved organic matter (fDOM). Meanwhile, we combined previously published brGDGT data (with 5- and 6-methyl brGDGTs separated) (Cao et al., 2020; Dang et al., 2018; Li et al., 2017; Martin et al., 2019; Martínez-Sosa et al., 2021; Miller et al., 2018; Ning et al., 2019; Qian et al., 2019; Russell et al., 2018; Stefanescu et al., 2021; Wang et al., 2021; Wu et al., 2021; Yao et al., 2020) to analyze their environmental response. Our aim was to investigate the distribution patterns and environmental response of brGDGTs in lakes on the TP to provide new insight into the mechanisms of GDGT-based indicators.

2. Materials and methods

2.1. Sampling

From 2009 to 2020, we investigated 83 lakes (average altitude, 4630 m) and collected 108 surface sediment samples and 22 surrounding soil samples during several field campaigns on the TP (Fig. 1). Among them, several samples from some large individual lakes were considered, whereas only one sample was retrieved from the center of the other lakes (Table S1). Surface sediment samples were obtained using an Ekman-Birge grab sampler at a sampling depth of 0 to <2 cm. To assess the source of archaeal tetraether in the lake sediments, 22 surface soil samples from 21 lake catchments were sampled (Table S2). Each sample was a combination of three random sub-samples (uppermost 5 cm) collected from different locations with intervals of tens of meters to represent the average soil condition of this location. All samples were placed in whirl-pak bags and stored in a freezer for further processing.

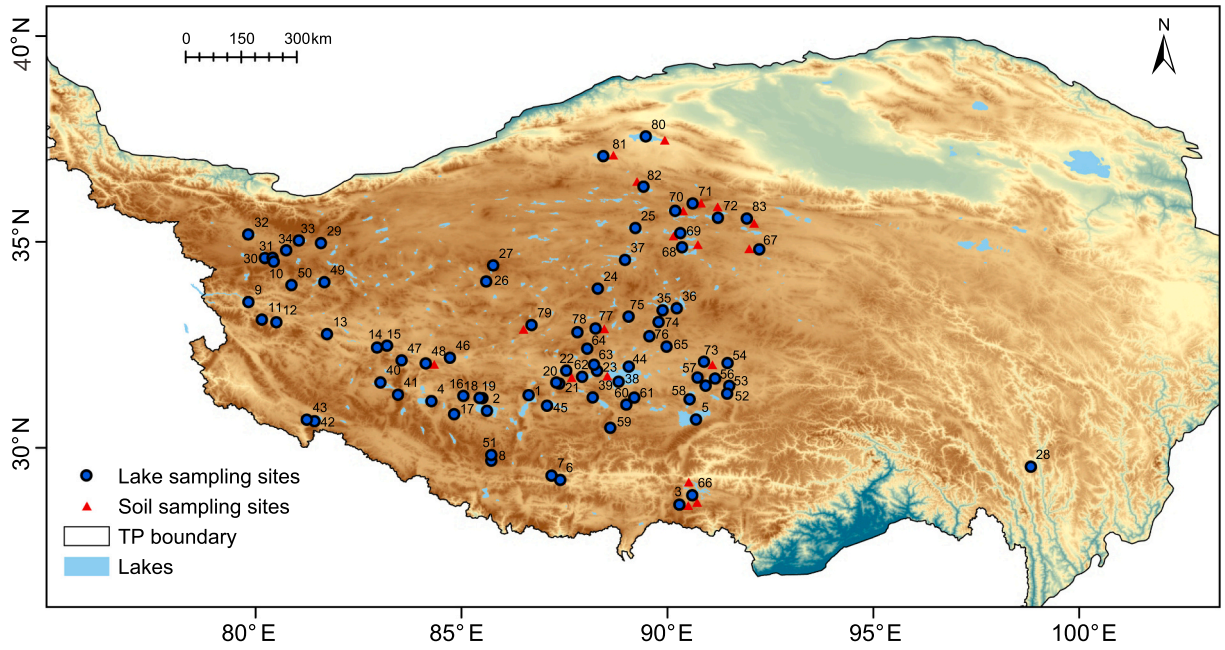

Fig. 1. Location of the 83 TP lakes (blue dots) and 22 surrounding soils (red triangles). (For interpretation of the references to colour in this figure legend, the reader is referred to the web version of this article.)

2.2. Environmental parameters

The in-situ water quality data of 83 lakes were measured using YSI EXO or HACH multi-parameter water quality instruments during fieldwork. Some relevant physical and chemical parameters of each lake have been presented previously (Liu et al., 2021). In the present study, water quality parameters mainly included salinity (in terms of total dissolved solids), DO, and pH. Notably, measurement data for some environmental variables, such as salinity, had great uncertainties. Although the sampling and water quality measurements were performed simultaneously and as far as possible in the geometric center of the lake to avoid the impact of heterogenous lake water quality, biomarkers in the sediment typically reflect an average signal of the past years or decades, and the measurement of water quality was equivalent to a "snapshot" during a lake survey. Therefore, the average environment conditions of the past years or decades are more reasonable as environmental variables. However, long-term and continuous monitoring data of lake environments on the TP are limited (Wang et al., 2020; Wang et al., 2019; Wang et al., 2014). Therefore, published water quality data were also collected, and the in-situ measurement data were averaged to minimize the bias caused by the above (Table S1). As expected, salinity and DO varied over several decades, which may be related to the rapid expansion or contraction of lakes in different areas of the TP (Zhang et al., 2020). Monthly air temperature data were extracted from the WorldClim 2.1 dataset, a high spatial resolution (~1 km^2) meteorological dataset, which contains data during the period of 1970 to 2000 (Fick and Hijmans, 2017). These data were used to calculate the mean annual air temperature (MAAT) and mean annual lake water temperature (MLWT). Of the two, MLWT was calculated based on Cao et al. (2020), in which the monthly air temperature was determined by assigning a value of 4 °C to the months with mean air temperatures of <4 °C.

2.3. Lipid analysis

The freeze-dried samples (4–10 g) were ultrasonically extracted with dichloromethane: methanol (9:1, *v*/v) to obtain the total lipid extract, which was concentrated using a rotary evaporator and saponified with 1 M KOH or MeOH solution (5% H_2O by volume) at 65 °C for 3 h. The neutral fraction was recovered by extraction with *n*-hexane (6 ×) and then separated into three fractions on an activated silica gel column by elution with *n*-hexane, dichloromethane, and methanol successively. The methanol fraction containing GDGTs needed to be filtered through a polytetrafluoroethylene filter (0.2 μm) prior to being analyzed.

GDGTs were analyzed using the Agilent 1260 series high-performance liquid chromatography-atmospheric pressure chemical ionization-mass spectrometer (HPLC-APCI-MS), equipped with an autosampler and ChemStation manager software. Samples were re-dissolved in *n*-hexane/ethyl acetate (84:16, v/v), and a known amount of internal C_{46} standard was added for quantification (Huguet et al., 2006). Separation of 5- and 6-methyl brGDGT isomers was achieved with three Hypersil Gold Silica LC columns in series (each 100 mm × 2.1 mm, 1.9 μm, Thermo Fisher Scientific, USA). The following conditions were used for HPLC: column temperature, 40 °C; injection volume, 20 μL; and flow rate 0.2 mL/min. *n*-Hexane and *n*-hexane/isopropanol (9:1, v/v) were employed as mobile phases A and B, respectively, and the elution gradient was as described by Yang et al. (2014) with some modifications. MS scanning was performed in selected ion monitoring mode that targeted specific $[M + H]^+$ ions at *m/z* 744 for the C_{46} standard, 653, 1302, 1300, 1298, 1296, and 1292 for the iGDGTs, and 1050, 1048, 1046, 1036, 1034, 1032, 1022, 1020, and 1018 for the brGDGTs. The 5-, 6-, 7-methyl, and unknown isomers of brGDGTs were assigned as described previously (De Jonge et al., 2014a; Ding et al., 2016; Wang et al., 2021). As is shown, the 5/6-methyl brGDGT isomer (IIIa'') is elute between 5- and 6-methyl isomers (Weber et al., 2015), while 7-methyl and unknown isomers (termed as IIIa''' and IIa''') are elute after 6-methyl isomers (Fig. S1). It should be noted that the naturally occurring isotopes of brGDGTs with $[M + H]^+$ at m/z 1048 and 1034 will contribute to the chromatograms of m/z 1050 and 1036, which may lead to the abundance of IIIa''' and IIa''' being overestimated. Therefore, in this study, the co-eluting isotope peaks in the chromatograms of m/z 1050 and 1036 were corrected by subtracting a response equal to 29% of their major peaks at m/z 1048 and 1034 according to theoretical isotope distributions (Wang et al., 2021). Since the quantification of brGDGTs assumes that their ionization efficiency is consistent with the internal standard, the final quantification was semi-quantitative.

2.4. Proxy calculations

The ACE and ACE' indexes were calculated with the following equations (He et al., 2020; Turich and Freeman, 2011):

ACE = archaeol / (archaeol + GDGT-0) × 100

ACE' = archaeol / (archaeol + 10 × brGDGTs) × 100

The MBT'$_{5ME}$ and MBT'$_{6ME}$ indexes were calculated based solely on 5- or 6-methyl brGDGTs (De Jonge et al., 2014a):

$$MBT'_{5ME} = (Ia + Ib + Ic)/(Ia + Ib + Ic + IIa + IIb + IIc + IIIa)$$

$$MBT'_{6ME} = (Ia + Ib + Ic)/(Ia + Ib + Ic + IIa' + IIb' + IIc' + IIIa')$$

The CBT$_{5ME}$ and CBT$_{6ME}$ indexes were calculated following the method of De Jonge et al. (2014a):

$$CBT_{5ME} = -^{10}log((Ib + IIb)/(Ia + IIa))$$

$$CBT_{6ME} = -^{10}log((Ib + IIb')/(Ia + IIa'))$$

The isomer ratio of 6- and 7-methyl (including 7-methyl and unknown isomers) brGDGTs was calculated with the following equation (De Jonge et al., 2015; Wang et al., 2021):

$$IR_{6ME} = (IIa' + IIb' + IIc' + IIIa' + IIIb' + IIIc')/(IIa + IIa' + IIb + IIb' + IIc + IIc' + IIIa + IIIa' + IIIb + IIIb' + IIIc + IIIc')$$

$$IR_{7ME} = (IIIa''' + IIa''')/(IIIa + IIIa' + IIIa''' + IIa + IIa' + IIa''')$$

$$IR_{6+7ME} = (IR_{6ME} + IR_{7ME})/2$$

$$IR'_{6+7ME} = (0.5 \times (IIa' + IIb' + IIc' + IIIa' + IIIb' + IIIc') + IIIa''' + IIa''')/(IIa + IIb + IIc + IIIa + IIIb + IIIc + IIa' + IIb' + IIc' + IIIa' + IIIb' + IIIc' + IIIa''' + IIa''')$$

2.5. Statistical analyses

The correlation matrix of brGDGT results and environmental variables was constructed using software SPSS statistics (version 22.0). Some variables (i.e., lake area, water depth, and salinity) were log-transformed to adjust for skewed distributions prior to these analyses. A *p*-value of <0.01 was considered significant. We used redundancy analyses (RDAs) to assess the influence of each environmental variable on the GDGT-based proxies, which was performed using the software Canoco (version 5.0). In general, a vertical projection of one arrow tip onto the other arrow line can be used to assess the correlations between related proxies and environmental factors. A strong correlation (positive in the acute angle and negative in the obtuse angle) depends on the distance of the projection point from the coordinate origin. Principal component analysis (PCA) identifies a set of orthogonal components that explain variations in the dataset and determines the degree to which each variable contributes to these components. PCA was performed using the Origin (version 2021b) software.

3. Results

3.1. Environmental parameters and distribution of brGDGTs

In this study, investigated lakes spanned a substantial range of salinity from 130 mg/L to 228,091 mg/L, and wide gradients of DO (0.15–11.7 mg/L); however, the pH range of these lakes was relatively narrow (7.0–10.5) (Table S1). Although the lakes had a wide MAAT range (−7.4 to 3.9 °C), the MLWT range was relatively narrow (4.0 to 7.1 °C).

Common brGDGTs occurred in all investigated lake sediments, with substantially varying concentrations (Table S2). The concentration of brGDGTs ranged from 0 to 408 ng g^{-1}, with a mean value of 18.23 ng g^{-1}. Pentamethylated brGDGTs (i.e., series II brGDGTs) constituted the largest fraction (44.9%) of the total brGDGT content in sediments of the investigated lakes, followed by hexamethylated (series III; 42.8%) and tetramethylated (series I; 11.4%) compounds. The 6-methyl brGDGTs were more abundant than 5-methyl isomers, which was reflected in the high IR$_{6ME}$ value, ranging from 0.33 to 0.98 with an average of 0.74. In addition, a series of isomers were observed in almost all samples, such as the 5/6-methyl isomer (i.e., brGDGTs-IIIa''; Weber et al., 2015), 7-methyl (i.e., brGDGTs-IIIa''', brGDGTs-IIa''' and unknown isomers) (Becker et al., 2013; Ding et al., 2016; Wang et al., 2021). The MBT values varied between 0.03 and 0.51 (average of 0.14), and CBT varied between −0.28 and 2.10 (average of 0.36).

3.2. Correlation matrix and redundancy analysis results

A correlation matrix was used to analyze the relationships between GDGT-based proxies and environmental parameters, including water depth, MAAT, MLWT, DO, salinity, and pH (Table S2). The environmental variables, such as pH and MAAT ($r = 0.55$, $p < 0.01$), DO and salinity ($r = -0.34$, $p < 0.01$), and salinity and pH ($r = -0.40$, $p < 0.01$) (Table S2) were correlated. For the brGDGT-based proxies, MBT'$_{5ME}$ showed a correlation with MAAT ($r = -0.29$, $p < 0.01$), while MBT'$_{6ME}$ and water depth were correlated ($r = -0.41$, $p < 0.01$); IR$_{6+7ME}$ was correlated with MAAT ($r = -0.33$, $p < 0.01$) and salinity ($r = 0.32$, $p < 0.01$). The total brGDGT concentration correlated well with MAAT ($r = 0.52$, $p < 0.01$) and salinity ($r = -0.55$, $p < 0.01$). For the iGDGT-based proxies, ACE was correlated with salinity ($r = 0.65$, $p < 0.01$) and water depth ($r = -0.43$, $p < 0.01$). Archaeol concentration was positively correlated with salinity ($r = 0.63$, $p < 0.01$), while caldarchaeol concentration was weakly correlated with water depth ($r = -0.33$, $p < 0.01$) and salinity ($r = -0.24$, $p < 0.05$).

RDA was then used to assess the impact of each environmental variable on the GDGT-based proxies. As shown in Fig. 2a, the brGDGT distribution was discrete, and the first two axes together explained only 16.72% of the brGDGT distribution data. The %6ME index was correlated with water depth ($r = 0.49$, $p < 0.01$). The common temperature proxy (MBT'$_{5ME}$) had no correlation with MAAT or MLWT, but was correlated with salinity. IR'$_{6+7ME}$ and IR$_{6+7ME}$ also correlated with salinity. In Fig. 2b, the first two axes accounted for 49.61% of the archaeal tetraether distribution data, and salinity appeared to be closely correlated with the Archaeol, ACE, and ACE' indices.

4. Discussion

4.1. Origin of GDGTs in TP lacustrine sediments

Identifying GDGT sources can improve the interpretation accuracy of GDGT-based environmental proxies (Blaga et al., 2009). Generally, there are two sources of GDGTs in lake sediments: in-situ lacustrine production and terrigenous soil origin. A previous study has confirmed that iGDGTs in the TP lakes of our study are primarily of autogenous origin (Kou et al., 2022). Although the overall distribution patterns of brGDGTs in soils are similar to those in lakes (i.e., hexamethylated

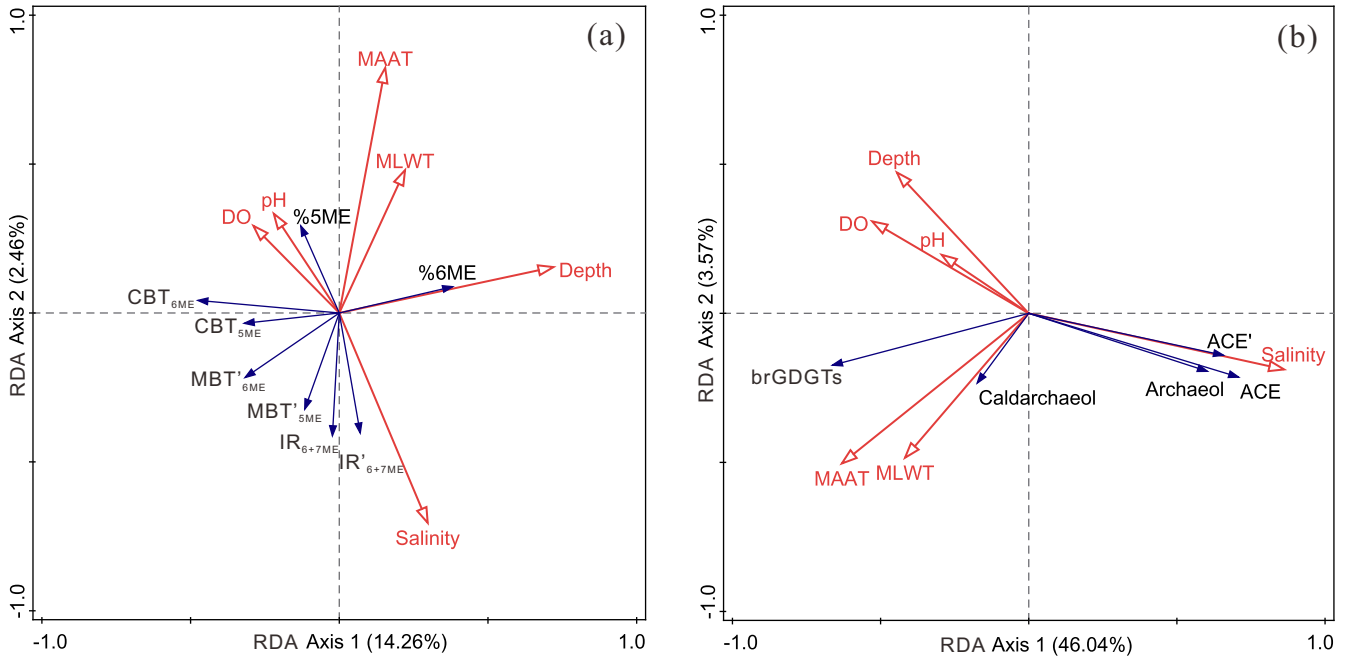

Fig. 2. RDA plots of (a) environmental variables (water depth, MAAT, MLWT, DO, pH, and salinity, red arrows) against brGDGT-based indicators (blue arrows) from the investigated lakes, and (b) environmental variables (water depth, MAAT, MLWT, DO, pH, and salinity, red arrows) against GDGT-based indicators (blue arrows). (For interpretation of the references to colour in this figure legend, the reader is referred to the web version of this article.)

brGDGTs are the highest abundance fractions in both lakes and soils), multiple lines of evidence suggest that lacustrine sedimentary brGDGTs on the TP are predominantly derived from in situ water column production. First, the brGDGT concentrations of lake sediments were apparently higher than those of the surrounding soils (Fig. 3a), suggesting a substantial contribution of in situ brGDGTs. In addition, the relative abundances of some brGDGT components (i.e., brGDGT-IIIa' and brGDGT-IIa') in the soils were markedly different from those in lake sediments (Fig. 3d). The soil brGDGT distribution showed more abundant brGDGT-IIIa' and brGDGT-IIa', which was consistent with the results of previous studies on the TP (Ding et al., 2015; Xiao et al., 2015). However, except for these two compounds, the other brGDGT fractional abundances in soils were lower than those in lake sediments (Fig. 3d). This contrast was also reflected in the fact that the MBT'$_{6ME}$ index in soils was significantly lower than that in lake sediments (Fig. 3b). Furthermore, the 5/6-methyl isomer compound (brGDGT-IIIa'') has been used as evidence of lake in-situ production (Cao et al., 2020; Weber et al., 2015; Weber et al., 2018). Similarly, the presence of brGDGT-IIIa'' in our investigated lakes but absence in surrounding soils may provide additional evidence for in situ production within the lakes (Fig. 3d).

There was a significantly high abundance of 6-methyl brGDGTs in both lake sediments and soils (Fig. 3d). Consistent with the soil brGDGT dataset of arid and semiarid regions (Dang et al., 2016; Ding et al., 2015; Xiao et al., 2015; Yang et al., 2015), the soil samples had a relatively high abundance of 6-methyl brGDGTs (reflected in the high IR$_{6ME}$ index) (Fig. 3c). However, lakes and surrounding soils had significant differences in terms of their IR$_{6ME}$ indices, indicating different biological sources in soil and lake settings (Fig. 3c). Meanwhile, the IR$_{6ME}$ index showed a clearly increasing trend with water depth, which further confirms the significantly autochthonous brGDGTs contributions from lakes (Fig. 3c). A study of lake vertical profiles has shown that 5- and 6-methyl brGDGTs may have different biological sources, and that the precursor microbes producing 6-methyl brGDGT prefer to inhabit oxygenated waters (Weber et al., 2018). It should be noted that most of our investigated lakes (accounting for 92%) do have an oxygen-rich environment (Kou et al., 2022). Therefore, combined with the above analysis, it can be inferred that the sedimentary brGDGTs in the investigated lakes were primarily produced in-situ.

Furthermore, we also performed a PCA and plotted a ternary diagram to evaluate the source of brGDGTs in our TP lakes (Fig. 4). It can be found that the overall brGDGT distribution of surrounding soils is more concentrated (except YZY11-1S, LC12S, PMY11S and CE12S, which are distributed across the entire distribution area of the lakes), and there are obvious differences among the lake sediments in terms of PCA (Fig. 4a). This further suggests that brGDGTs in the most of lake sediments were mainly derived from an autogenous origin. However, we also observed some overlap of brGDGT distributions between lake sediments and surrounding soils, especially for certain samples (e.g., Wulanwula Lake, Hoh Xil Lake, Baidoi Co, and Yagain Co) that coincided with the distribution of lakes (Fig. 4a and b). This may imply that terrestrial inputs cannot be completely ignored, at least for some lakes. Certainly, regional differences may also contribute to this phenomenon due to the circumstance that our soil sample sites did not cover all the lake basins. Generally, suspended particle matter (SPM) which filtered from lake water is an effective means for assessing the source of sedimentary brGDGTs (Buckles et al., 2014). Unfortunately, our investigated samples do not contain SPM, and therefore could not be used to accurately judge the contribution proportion of terrigenous input. In summary, despite some remaining complexity, the evidence of in-situ lacustrine brGDGTs development was clear and significant in most of our investigated lakes. Therefore, we infer that sedimentary brGDGTs of our investigated lakes are mainly of autogenous origin, followed by terrigenous input.

4.2. *Influence of salinity on brGDGT-based temperature indicators*

Temperature is one of the most important environmental factors affecting the distribution of brGDGTs (Schouten et al., 2013); however, the temperature response of brGDGTs varies depending on the research areas or carriers. Thus, many local and global calibrations have been presented to improve its application with the old analytical method in lacustrine settings (Loomis et al., 2012; Pearson et al., 2011; Sun et al., 2011; Tierney et al., 2010) and the new method (i.e., effectively separating 5-methyl and 6-methyl isomers) (Dang et al., 2018; Martínez-Sosa et al., 2021; Russell et al., 2018; Wang et al., 2021). The separation of

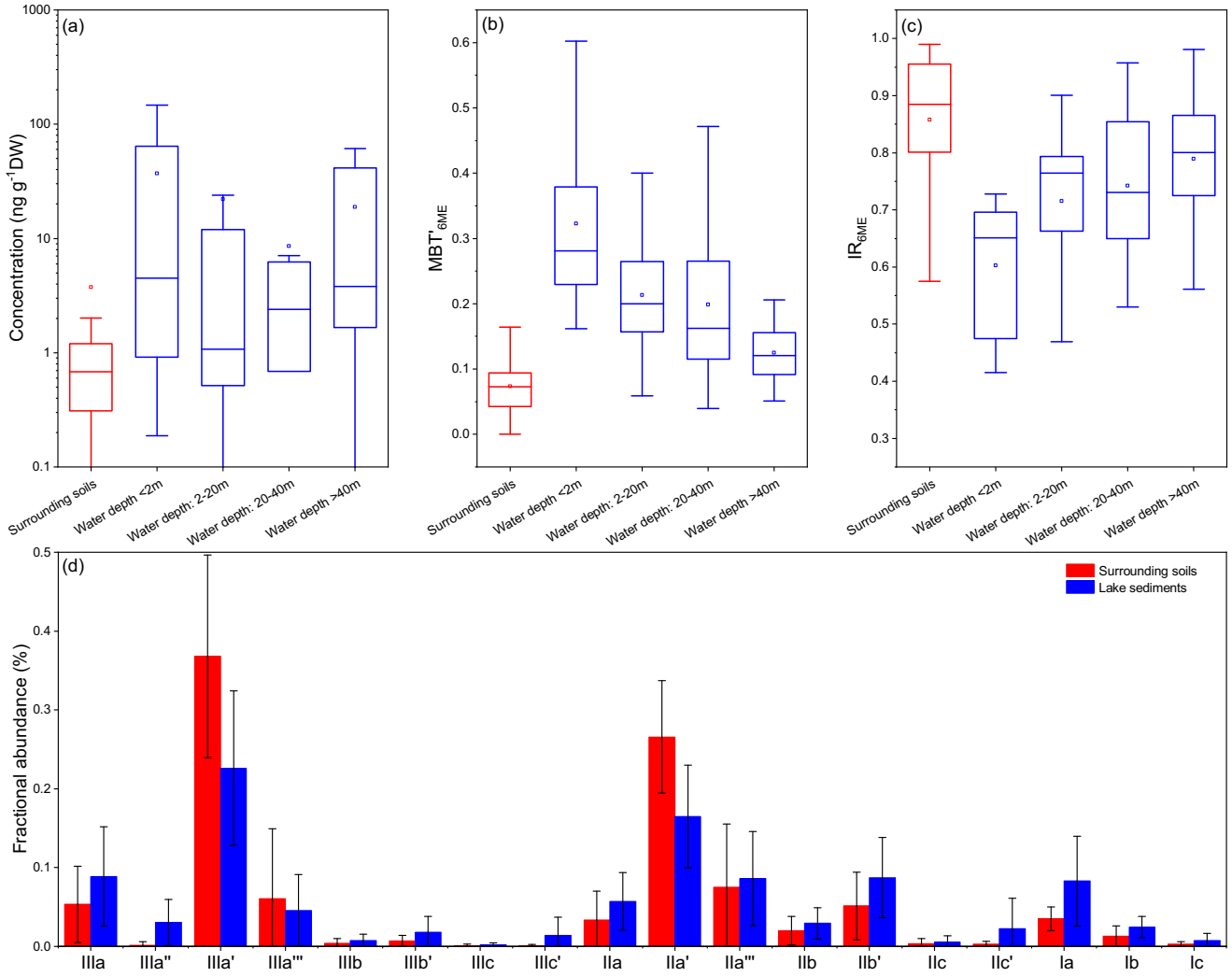

Fig. 3. Comparison of brGDGTs distributions within lake surface sediments and surrounding soils. Box plots showing the values of (a) brGDGTs concentration, (b) MBT'$_{6ME}$, and (c) IR$_{6ME}$. The dots in the boxes are mean values. The average distributions of brGDGTs from lake surface sediments and surrounding soils are shown in (d).

isomers clarifies the environmental response signal of brGDGTs (Dang et al., 2016; De Jonge et al., 2014a). However, there are some contradictions, such as MBT'$_{6ME}$ responding to temperature in East Asian lakes (Dang et al., 2018; Qian et al., 2019) and MBT'$_{5ME}$ responding to temperature in East African lakes (Russell et al., 2018). A recent study has shown that salinity has a significant impact on MBT'$_{5ME}$ (Wang et al., 2021). According to our survey of TP environmental data, the lake pH and MLWT gradients were shallow, while the salinity gradient was steep (see Section 2.2). Therefore, we combined the global lake datasets (Cao et al., 2020; Dang et al., 2018; Li et al., 2017; Martin et al., 2019; Martínez-Sosa et al., 2021; Miller et al., 2018; Ning et al., 2019; Qian et al., 2019; Russell et al., 2018; Stefanescu et al., 2021; Wang et al., 2021; Wu et al., 2021; Yao et al., 2020) and divided them into three categories to test the MBT'$_{5ME}$ and MBT'$_{6ME}$ responses to temperature: freshwater lakes (salinity ≤1000 mg/L), brackish lakes (1000 mg/L < salinity <35,000 mg/L), and saline lakes (salinity ≥35,000 mg/L).

The results showed that lake salinity had a noticeable effect on the brGDGT-based temperature indicators. MBT'$_{5ME}$ had the best correlation with temperature in freshwater lakes (Fig. 5a; $r^2 = 0.85$, $p < 0.01$), whereas MBT'$_{6ME}$ had a good correlation with temperature in saline lakes (Fig. 5f; $r^2 = 0.49$, $p < 0.01$). However, for brackish lakes, neither MBT'$_{5ME}$ nor MBT'$_{6ME}$ exhibited a weak correlation with temperature (Fig. 5b and e). The reason for the different responses of MBT'$_{5ME}$ and MBT'$_{6ME}$ to temperature has not been determined, but increasing evidences have shown that the bacterial communities producing 5- and 6-methyl brGDGTs are likely to be different (De Jonge et al., 2019; Weber et al., 2018). Analysis based on the global lacustrine brGDGTs database demonstrated that the MBT'$_{5ME}$ calculation was not applicable to highly alkaline, hypersaline systems (Martínez-Sosa et al., 2021). The unique feature of the strong predominance of 6-methyl brGDGTs in the Mariana Trench was also deemed to be the effect of authigenic biogenic sources in alkaline seawater and low subsurface temperatures (Xiao et al., 2020). Our results seemed to further corroborate the difference in biological sources between freshwater and high-salinity environments. MBT'$_{6ME}$ may be more suitable to represent the temperature in a high-salinity environment, which strongly predominates 6-methyl brGDGTs. The weak correlation between MBT'$_{5/6ME}$ and temperature in brackish lakes might be due to a mixed effect from the different microbial communities responding to temperature (i.e., preferentially fresh- or saltwater-dominated microbial communities).

In summary, we emphasize the impact of salinity on brGDGT-based temperature indicators, and MBT'$_{5ME}$ can be used as a robust temperature proxy in freshwater lakes, while MBT'$_{6ME}$ is more suitable in saline lakes. Therefore, investigating and evaluating the lake environment before using these temperature proxies is crucial. In contrast, the change of possible biogenic sources caused by this salinity will also bring great

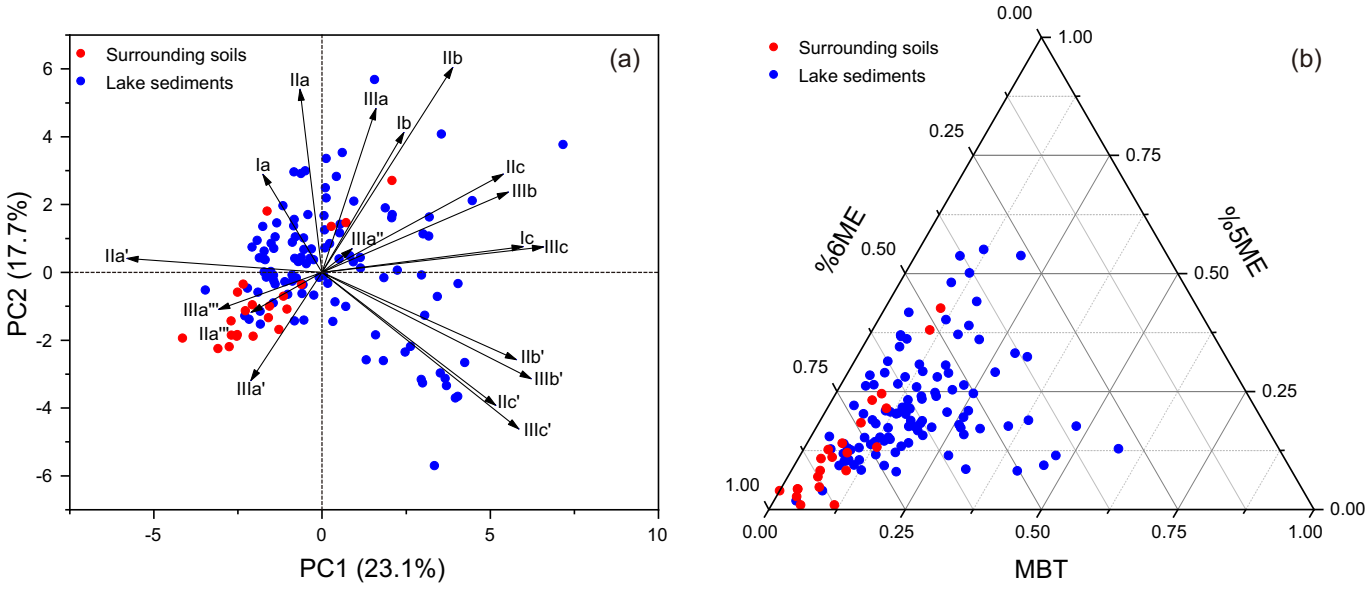

Fig. 4. (a, b) Principal component analysis (PCA) and ternary diagram showing the brGDGT distributions in our study lakes and surrounding soils.

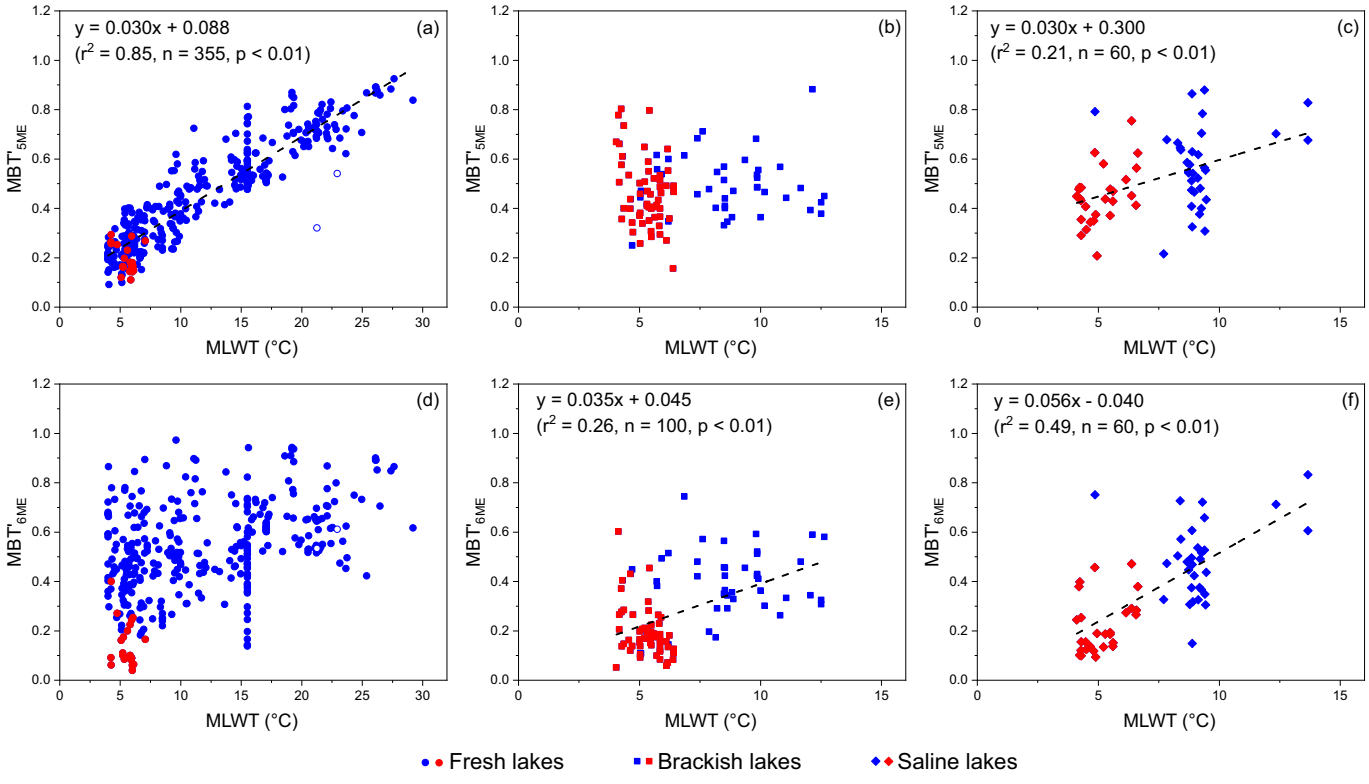

Fig. 5. Relationships between brGDGT-based temperature indicators and MLWT for global lakes in different salinity range. (a)–(c) MBT'$_{5ME}$ and MLWT, (d)–(f) MBT'$_{6ME}$ and MLWT. Circles represent fresh lakes, squares represent brackish lakes, rhomboids represent saline lakes. Global lakes from previous studies (blue) (Cao et al., 2020; Dang et al., 2018; Li et al., 2017; Martin et al., 2019; Martínez-Sosa et al., 2021; Miller et al., 2018; Ning et al., 2019; Qian et al., 2019; Russell et al., 2018; Stefanescu et al., 2021; Wang et al., 2021; Wu et al., 2021; Yao et al., 2020) and this work (red). Hollow circles in (a) and (d) indicate the outlier lakes (two freshwater lakes) excluded from temperature regressions. Dead Sea data from Martínez-Sosa et al. (2021) is not included in our global lake dataset due to that lake's values being outside the range of environmental parameters for most of our lake sample databases. (For interpretation of the references to colour in this figure legend, the reader is referred to the web version of this article.)

uncertainty to our paleotemperature reconstruction using this index. This effect is more obvious in brackish lakes from arid and semi-arid areas because these areas often have large hydrologic/salinity fluctuations during paleoclimate evolution. Therefore, paleotemperature reconstruction using MBT'$_{5ME}$ needs to be cautious for brackish lakes. For saline lakes, we suggest that MBT'$_{6ME}$ may be an available temperature proxy.

4.3. Assessment of the GDGT-based indicators as salinity proxy

Salinity has an important effect on microbial community structure (Benlloch et al., 2002; Jiang et al., 2009; Jiang et al., 2006; Yang et al., 2019). Halophilic Euryarchaeota, which mainly synthesize archaeol (Dawson et al., 2012; Macalady et al., 2004), usually dominate the archaeal community in hypersaline environments (Jiang et al., 2006; Pancost et al., 2011); however, the caldarchaeol precursors (Crenarchaeota, Thaumarchaeota, and some species of Euryarchaeota) can survive and thrive over a broad salinity range (Macalady et al., 2004; Turich and Freeman, 2011). Based on this, the ACE index was proposed as a salinity proxy (Turich and Freeman, 2011). Previous studies on northeastern TP lakes have shown a significant correlation between ACE and salinity in lake sediments and SPM (Wang et al., 2013) and the complexity of this relationship has been noted (Günther et al., 2014; Li et al., 2016). In this study, the ACE index was further confirmed to be significantly correlated with salinity ($r^2 = 0.46$, $n = 105$, $p < 0.01$, Fig. 6a). Meanwhile, several anomalies were also found (i.e., two abnormally low values, Longmu Lake and Jieze Caka; two abnormally high values, Longwe Lake and Dogaicorng Qangco). If these four outliers were excluded, the correlation with salinity was significantly improved ($r^2 = 0.71$, $n = 101$, $p < 0.01$). The cause of these anomalies is not clear at present. We speculate that it may be related to the oxygen content (Weber et al., 2018; Wu et al., 2021; Yao et al., 2020) or environmental conditions of the lake itself (e.g., the existence of hot springs in Dogaicorng Qangco, and extremely high salinity in Longmu Lake and Jieze Caka). Nevertheless, our results support that ACE has the potential to be a reliable salinity proxy in TP lakes. Furthermore, it was observed that ACE index and archaeal concentrations remained low in the range of low salinity (freshwater and brackish lakes) and did not change significantly until a higher salinity threshold was reached. This is reasonable because the ACE index is driven by changes in archaeal communities. Generally, archaeal communities change only when salinity reaches a certain threshold. He et al. (2020) identified a threshold for the ACE index (salinity = ~60,000 mg/L) from an investigation of mid-latitude Asian lakes, while the threshold seems lower (salinity = ~40,000 mg/L) in the present study. Nevertheless, the high response threshold of ACE index may limit its application in paleosalinity reconstruction, and it can only record the history of significant salinity/hydrological fluctuation. Furthermore, for the TP region, lake hydrology tends to vary greatly (Zhang et al., 2020), which results in large salinity fluctuations. For instance, salinity data collected on the TP over the past several decades has shown significant changes in lake salinity, especially for small lakes with shallow water (Table S1). This may be related to the rapid expansion or shrinkage of the lakes. A negative correlation between brGDGT concentration and salinity ($r^2 = 0.31$, $n = 108$) was observed (Fig. S2), indicating that salinity inhibits the growth of bacteria. Accordingly, He et al. (2020) proposed the ACE' index, which replaced the caldarchaeol with brGDGTs, and found a slightly better correlation with salinity. Compared with the ACE index, the correlation between ACE' and salinity is slightly improved, and there is less dispersion in the low salinity range, indicating its potential as a novel salinity proxy. Our results support their findings that ACE' could be used as a novel salinity proxy; however, its correlation with salinity was not improved in TP lakes ($r^2 = 0.37$, $n = 105$, $p < 0.01$) (Fig. 6b). This may be related to the mixed influence of various environmental factors on brGDGTs (e.g., salinity, temperature, and water depth can also affect the distribution of brGDGTs in our dataset). Therefore, to improve the applicability of the ACE' index, more databases are required to be modified to improve the accuracy. In summary, both ACE and ACE' can change with a large salinity fluctuation of ~3000 to 100,000 mg/L (Fig. 6a and b), and such a large fluctuation may occur in some arid and semi-arid regions during glacial and interglacial periods or drought events.

In addition, in our dataset, lake salinity showed a significant impact on the distribution of sedimentary brGDGTs, especially the relative abundance of brGDGT isomers (including IIIa'' and IIa''), which was reflected in the IR_{6ME} and IR_{7ME} indices. However, the sensitivities of these two proxies to salinity were different. IR_{6ME} showed a significant correlation with salinity in both the TP freshwater lake ($r^2 = 0.61$, $n = 22$, $p < 0.01$) and global databases ($r^2 = 0.50$, $n = 209$, $p < 0.01$) (Fig. 6c); however, there was no correlation in brackish and saline lakes (Fig. 6c). In contrast, IR_{7ME} was correlated with lake salinity on the TP and other brackish and saline lakes around the world ($r^2 = 0.26$, $n = 150$, $p < 0.01$) (Fig. 6d), while there was no relationship with salinity in fresh lakes (Fig. 6d). This was consistent with the results of a previous study (Wang et al., 2021). However, the mechanism of salinity response remains unclear. According to a study on soil brGDGT, pH is the dominant factor controlling isomerization (De Jonge et al., 2014a), and thus, salinity might indirectly affect the isomerization index through pH in lake systems. However, it is difficult to establish this. In contrast, most of the lakes we investigated were alkaline (pH > 7), and there was little change in pH (Table S1). Although pH was correlated with salinity ($r = -0.40$, $p < 0.01$), the correlation between pH and IR_{6ME} ($r = -0.45$, $p < 0.05$) was much lower than that between salinity and IR_{6ME} ($r = 0.78$, $p < 0.01$) in our study of fresh lakes. However, controlled lacustrine microcosms also reveal that pH does not affect IR_{6ME} (Martínez-Sosa et al., 2020). Thus, salinity may directly affect brGDGT isomerization. Furthermore, Wu et al. (2021) found that the relative abundance of 6-methyl brGDGTs exhibits a stepwise decline with DO concentration in Lake Yangzonghai. This indicates that DO concentration may also be one of the factors affecting IR_{6ME}; however, more research is needed to confirm this since there are few related studies. Based on current global brGDGTs data, IR_{6ME} has the potential to be a sensitive proxy for salinity in freshwater lakes. However, its applicability is limited. This is because the salinity of lakes, especially temperate lakes, varies greatly and is usually beyond the scope of application of IR_{6ME}. Accordingly, the new proposed indices (IR_{6+7ME} and IR'_{6+7ME}), which combine IR_{6ME} and IR_{7ME}, could overcome this issue and are suitable for the entire salinity range (Wang et al., 2021). For our TP lakes, both indices show the correlation with salinity ($r^2 = 0.35$ for IR_{6+7ME} and $r^2 = 0.36$ for IR'_{6+7ME}), and the correlation was stronger when combined with the global lake database (Fig. 6e and f) ($r^2 = 0.63$ for IR_{6+7ME} and $r^2 = 0.64$ for IR'_{6+7ME}). They still maintain good correlation in different salinity ranges (Fig. S3), so it can be inferred that these indices may represent novel salinity proxies.

4.4. Implications for paleotemperature and paleosalinity reconstruction

As mentioned above, the response of MBT'_{5Me} and MBT'_{6Me} to temperature has regional differentiation (Dang et al., 2018; Qian et al., 2019; Russell et al., 2018) and is most likely due to differences in the bacterial communities that produce 5- and 6-methyl brGDGTs (De Jonge et al., 2019; Weber et al., 2018). Our results support this view and suggest that salinity is one of the dominating factors in controlling bacterial community change. Taking into consideration the global lake database, we propose that MBT'_{5ME} is suitable for paleotemperature reconstruction of freshwater lakes, while MBT'_{6ME} is more suitable for high salinity lakes (i.e., salinity ≥35,000 mg/L). However, these varied responses will still cause uncertainty in brGDGT-based paleotemperature reconstructions. This uncertainty may cause little effect on paleotemperature records in the lakes in humid regions with high precipitation, but it could considerably influence lake sediment records in arid and semi-arid regions where the paleosalinity of lakes commonly fluctuates greatly. Thus, it is necessary to ensure that there is no significant change in lake salinity during the paleotemperature reconstruction using a single MBT'_{5ME} index. If there is a significant change in lake salinity at a certain period (e.g., the lake changes from freshwater to salt water), the reconstructed paleotemperature with MBT'_{5ME} may be inaccurate for that period. Therefore, we suggest that the $MBT'_{5/6ME}$ paleothermometer should be used carefully in areas with large salinity fluctuation (especially TP), and it is essential to evaluate the applicable conditions of these two proxies before paleotemperature reconstruction.

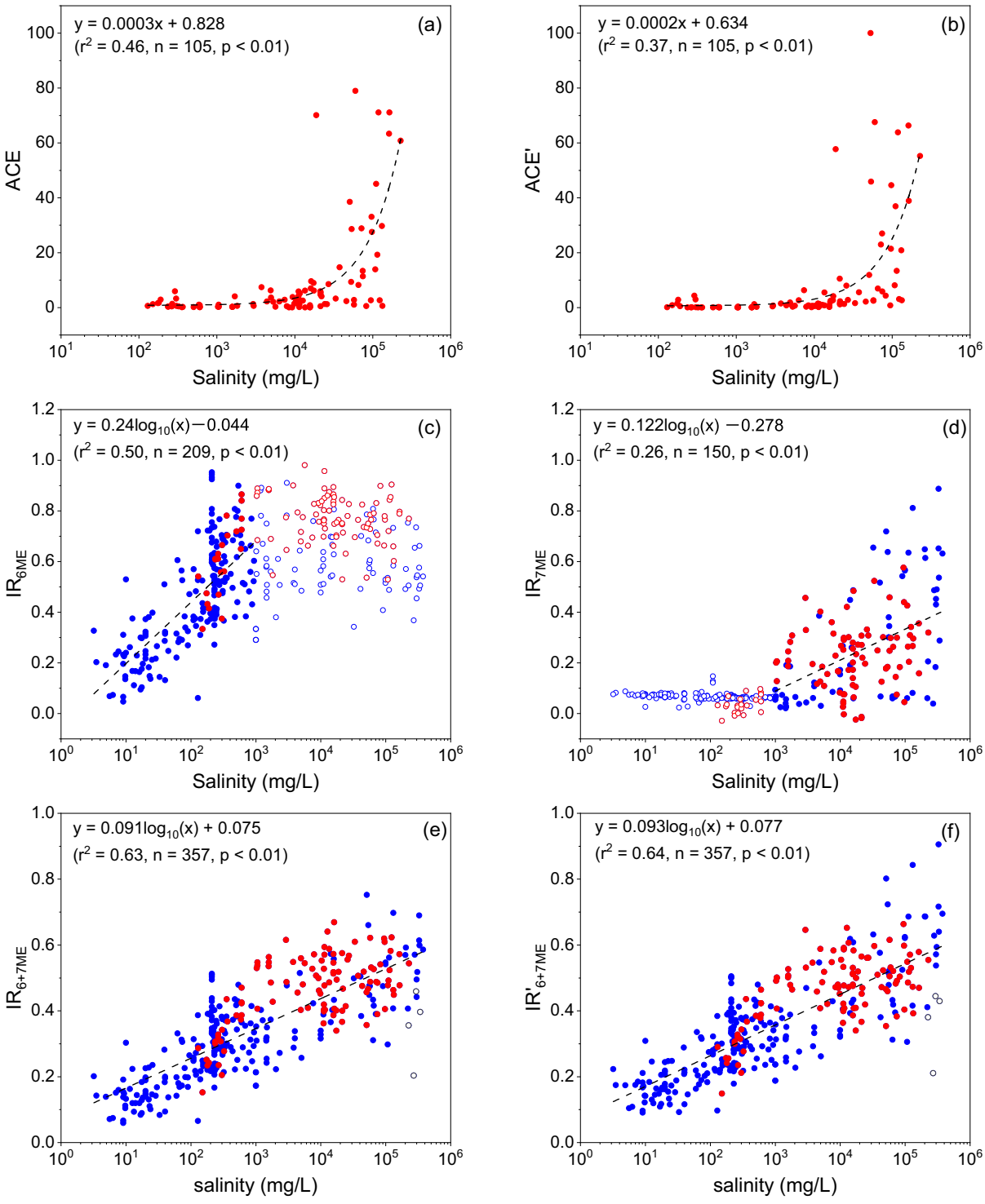

Fig. 6. Relationships between GDGT-based indicators and salinity for global lakes. (a) ACE, (b) ACE', (c) IR_{6ME}, (d) IR_{7ME}, (e) IR_{6+7ME} and (f) IR'_{6+7ME} against lake salinity. Data from previous studies (Cao et al., 2020; Dang et al., 2018; Li et al., 2017; Martin et al., 2019; Martínez-Sosa et al., 2021; Miller et al., 2018; Ning et al., 2019; Qian et al., 2019; Russell et al., 2018; Stefanescu et al., 2021; Wang et al., 2021; Wu et al., 2021; Yao et al., 2020) and this work. The red hollow/solid dots represent this study, blue hollow/solid dots represent global lakes. Black hollow dots in (c)–(d) indicate that are excluded from regressions. Dead Sea data from Martínez-Sosa et al. (2021) is not included in our global lake dataset due to that lake's values being outside the range of environmental parameters for most of our lake sample databases. Note that since brGDGTs-IIIa''' and brGDGTs-IIa''' are rarely reported in previous global lake brGDGT dataset, we calculated these two compounds based on the rule proposed by Wang et al. (2021), which assumes that the relative abundance of these isomers to 5-methyl and 6-methyl brGDGTs is similar to the average values of mid-latitude freshwater lakes. (For interpretation of the references to colour in this figure legend, the reader is referred to the web version of this article.)

As for salinity proxies, our TP lake database further confirmed the potential of ACE and the recently proposed ACE' to reconstruct paleosalinity. Therefore, we suggest that the ACE index can be used as a lake salinity proxy in the TP area; however, due to a flaw in the index (i.e., the high response threshold), it can only respond to large hydrological and salinity fluctuations and cannot reflect continuous changes in lake salinity. In contrast, IR_{6+7ME} and IR'_{6+7ME} indexes were sensitive to salinity and covered different salinity ranges and may represent novel salinity proxies. In summary, combining ACE (ACE') and IR'_{6+7ME} (IR_{6+7ME}) indices is suggested for the reconstruction of lake paleosalinity, so that the two indexes can be mutually verified and ultimately provide more reliable salinity records.

5. Conclusions

The investigation of the variations in GDGT abundance and distribution in 108 lake sediment and 22 surrounding soils sample sites for 83 lakes on the TP identified that sedimentary brGDGTs were mainly produced in-situ. Combined with published brGDGT data from other lakes across the globe, we found that MBT'_{5ME} and MBT'_{6ME} have different responses to temperature in different salinity ranges, i.e., MBT'_{5ME} showed the best correlation with temperature in freshwater lakes, and MBT'_{6ME} showed a better correlation with temperature in saline lakes; however, both indices showed a poor correlation in brackish lakes. This finding may be important for paleotemperature reconstruction, since typically only a single temperature proxy is selected for this technique. Therefore, we suggest that the application of brGDGT-based temperature proxies to lakes with large salinity fluctuations should be treated with caution. These different response strategies imply that the biological communities producing 5- and 6-methyl brGDGTs are likely to be different, and that a predominance of 6-methyl brGDGTs may be synthesized in high-salinity environments. This assumption might be addressed in future studies. In addition, we assessed the applicability of salinity indicators on the TP based on brGDGT and iGDGTs. In agreement with previous studies, both IR'_{6+7ME} (IR_{6+7ME}) and ACE (ACE') can respond to lake salinity in the TP, and have the potential as proxies for paleosalinity. However, ACE (ACE') may only record the history of significant salinity/hydrological fluctuation due to its high salinity response threshold. The integration of ACE and IR'_{6+7ME} can provide a reliable record of paleosalinity/paleohydrology fluctuations. This study highlights the influence of salinity on GDGT-based indicators and the potential of brGDGTs in reconstructing both lake salinity and temperature changes in lacustrine sedimentary archives.

Declaration of Competing Interest

We declare that we have no known competing financial interests or personal relationships that could have appeared to influence the work reported in this paper.

Acknowledgements

We would like to thank Drs. Chong Liu, Xiao Lin, Yong Wang, Baojin Qiao, Run Zhang, Hao Chen, Mr. Jinlei Kai and Baolong Du, and Ms. Siwei Yu for the fieldwork, Lei Zhang for extracting the meteorological data, Jie Wu and Hongye Pei for helpful discussion, Shaopeng Gao for help with LC-MS maintenance. We also thank the two anonymous reviewers for their helpful comments and suggestions. This study is co-supported by the Second Tibetan Plateau Scientific Expedition and Research Program (STEP) (2019QZKK0202), the National Natural Science Foundation of China project (grant number 41831177) and Chinese Academy of Sciences Strategic Priority Research Program (grant number XDA20020100).

Appendix A. Supplementary data

Supplementary data to this article can be found online at https://doi.org/10.1016/j.palaeo.2022.111127.

References

An, Z., Kutzbach, J.E., Prell, W.L., Porter, S.C., 2001. Evolution of Asian monsoons and phased uplift of the Himalaya–Tibetan plateau since Late Miocene times. Nature. 411 (6833), 62–66.
Becker, K.W., Lipp, J.S., Zhu, C., Liu, X., Hinrichs, K.U., 2013. An improved method for the analysis of archaeal and bacterial ether core lipids. Org. Geochem. 61, 34–44.
Benlloch, S., Lopez-Lopez, A., Casamayor, E.O., Ovreas, L., Goddard, V., Daae, F.L., Smerdon, G., Massana, R., Joint, I., Thingstad, F., Pedros-Alio, C., Rodriguez-Valera, F., 2002. Prokaryotic genetic diversity throughout the salinity gradient of a coastal solar saltern. Environ. Microbiol. 4 (6), 349–360.
Blaga, C.I., Reichart, G.J., Heiri, O., Damste, J.S.S., 2009. Tetraether membrane lipid distributions in water-column particulate matter and sediments: a study of 47 European lakes along a north-south transect. J. Paleolimnol. 41 (3), 523–540.
Buckles, L.K., Weijers, J.W.H., Verschuren, D., Sinninghe Damsté, J.S., 2014. Sources of core and intact branched tetraether membrane lipids in the lacustrine environment: Anatomy of Lake Challa and its catchment, equatorial East Africa. Geochim. Cosmochim. Acta 140, 106–126.
Cao, J., Rao, Z., Shi, F., Jia, G., 2020. Ice formation on lake surfaces in winter causes warm-season bias of lacustrine brGDGT temperature estimates. Biogeosciences. 17 (9), 2521–2536.
Castañeda, I.S., Schouten, S., 2011. A review of molecular organic proxies for examining modern and ancient lacustrine environments. Quat. Sci. Rev. 30 (21), 2851–2891.
Chen, J., Chen, F., Zhang, E., Brooks, S.J., Zhou, A., Zhang, J., 2009. A 1000-year chironomid-based salinity reconstruction from varved sediments of Sugan Lake, Qaidam Basin, arid Northwest China, and its palaeoclimatic significance. Sci. Bull. 54 (20), 3749–3759.
Dang, X., Yang, H., Naafs, B.D.A., Pancost, R.D., Xie, S., 2016. Evidence of moisture control on the methylation of branched glycerol dialkyl glycerol tetraethers in semi-arid and arid soils. Geochim. Cosmochim. Acta 189, 24–36.
Dang, X., Ding, W., Yang, H., Pancost, R.D., Naafs, B.D.A., Xue, J., Lin, X., Lu, J., Xie, S., 2018. Different temperature dependence of the bacterial brGDGT isomers in 35 Chinese lake sediments compared to that in soils. Org. Geochem. 119, 72–79.
Dawson, K.S., Freeman, K.H., Macalady, J.L., 2012. Molecular characterization of core lipids from halophilic archaea grown under different salinity conditions. Org. Geochem. 48, 1–8.
De Jonge, C., Hopmans, E.C., Stadnitskaia, A., Rijpstra, W.I.C., Hofland, R., Tegelaar, E., Damste, J.S.S., 2013. Identification of novel penta- and hexamethylated branched glycerol dialkyl glycerol tetraethers in peat using HPLC-MS2, GC-MS and GC-SMB-MS. Org. Geochem. 54, 78–82.
De Jonge, C., Hopmans, E.C., Zell, C.I., Kim, J.H., Schouten, S., Damste, J.S.S., 2014a. Occurrence and abundance of 6-methyl branched glycerol dialkyl glycerol tetraethers in soils: Implications for palaeoclimate reconstruction. Geochim. Cosmochim. Acta 141, 97–112.
De Jonge, C., Stadnitskaia, A., Hopmans, E.C., Cherkashov, G., Fedotov, A., Damste, J.S.S., 2014b. In situ produced branched glycerol dialkyl glycerol tetraethers in suspended particulate matter from the Yenisei River, Eastern Siberia. Geochim. Cosmochim. Acta 125, 476–491.
De Jonge, C., Stadnitskaia, A., Fedotov, A., Sinninghe Damsté, J.S., 2015. Impact of riverine suspended particulate matter on the branched glycerol dialkyl glycerol tetraether composition of lakes: the outflow of the Selenga River in Lake Baikal (Russia). Org. Geochem. 83-84, 241–252.
De Jonge, C., Radujkovic, D., Sigurdsson, B.D., Weedon, J.T., Janssens, I., Peterse, F., 2019. Lipid biomarker temperature proxy responds to abrupt shift in the bacterial community composition in geothermally heated soils. Org. Geochem. 137, 103897.
Ding, S., Xu, Y., Wang, Y., He, Y., Hou, J., Chen, L., He, J., 2015. Distribution of branched glycerol dialkyl glycerol tetraethers in surface soils of the Qinghai–Tibetan Plateau: implications of brGDGTs-based proxies in cold and dry regions. Biogeosciences. 12 (11), 3141–3151.
Ding, S., Schwab, V.F., Ueberschaar, N., Roth, V.N., Lange, M., Xu, Y., Gleixner, G., Pohnert, G., 2016. Identification of novel 7-methyl and cyclopentanyl branched glycerol dialkyl glycerol tetraethers in lake sediments. Org. Geochem. 102, 52–58.
Feakins, S.J., Wu, M.S., Ponton, C., Tierney, J.E., 2019. Biomarkers reveal abrupt switches in hydroclimate during the last glacial in southern California. Earth Planet. Sc Lett. 515, 164–172.
Fick, S.E., Hijmans, R.J., 2017. WorldClim 2: new 1-km spatial resolution climate surfaces for global land areas. Int. J. Climatol. 37 (12), 4302–4315.
Gambacorta, A., Gliozzi, A., Derosa, M., 1995. Archaeal lipids and their biotechnological applications. World J. Microbiol. Biotechnol. 11 (1), 115–131.
Gasse, F., 2002. Diatom-inferred salinity and carbonate oxygen isotopes in Holocene waterbodies of the western Sahara and Sahel (Africa). Quat. Sci. Rev. 21 (7), 737–767.
Günther, F., Thiele, A., Gleixner, G., Xu, B., Yao, T., Schouten, S., 2014. Distribution of bacterial and archaeal ether lipids in soils and surface sediments of Tibetan lakes: Implications for GDGT-based proxies in saline high mountain lakes. Org. Geochem. 67, 19–30.
He, Y., Wang, H., Meng, B., Li, H., Zho, A., Song, M., Kolpakova, M., Kriyonogov, S., Liu, W., Liu, Z., 2020. Appraisal of alkenone- and archaeal ether-based salinity indicators in mid-latitude Asian lakes. Earth Planet. Sc Lett. 538.

Heinrichs, M.L., Walker, I.R., 2006. Fossil midges and palaeosalinity: potential as indicators of hydrological balance and sea-level change. Quat. Sci. Rev. 25 (15–16), 1948–1965.
Huguet, A., Grossi, V., Belmahdi, I., Fosse, C., Derenne, S., 2015. Archaeal and bacterial tetraether lipids in tropical ponds with contrasting salinity (Guadeloupe, French West Indies): Implications for tetraether-based environmental proxies. Org. Geochem. 83-84, 158–169.
Huguet, C., Hopmans, E.C., Febo-Ayala, W., Thompson, D.H., Damste, J.S.S., Schouten, S., 2006. An improved method to determine the absolute abundance of glycerol dibiphytanyl glycerol tetraether lipids. Org. Geochem. 37 (9), 1036–1041.
Jiang, H., Dong, H., Zhang, G., Yu, B., Chapman, L., Fields, M., 2006. Microbial diversity in water and sediment of Lake Chaka, an athalassohaline lake in northwestern China. Appl. Environ. Microbiol. 72 (6), 3832–3845.
Jiang, H., Dong, H., Deng, S., Yu, B., Huang, Q., Wu, Q., 2009. Response of Archaeal Community Structure to Environmental changes in Lakes on the Tibetan Plateau, Northwestern China. Geomicrobiol J. 26 (4), 289–297.
Ju, J., Zhu, L., Wang, J., Xie, M., Zhen, X., Wang, Y., Peng, P., 2010. Water and sediment chemistry of Lake Pumayum Co, South Tibet, China: implications for interpreting sediment carbonate. J. Paleolimnol. 43, 463–474.
Kou, Q., Zhu, L., Ma, Q., Wang, J., Ju, J., Xu, T., Liu, C., Li, C., Kai, J., 2022. Distribution, potential sources, and response to water depth of archaeal tetraethers in Tibetan Plateau lake sediments. Chem. Geol. 601, 120825.
Li, J., Pancost, R.D., Naafs, B.D.A., Yang, H., Zhao, C., Xie, S., 2016. Distribution of glycerol dialkyl glycerol tetraether (GDGT) lipids in a hypersaline lake system. Org. Geochem. 99, 113–124.
Li, J., Naafs, B.D.A., Pancost, R.D., Yang, H., Liu, D., Xie, S., 2017. Distribution of branched tetraether lipids in ponds from Inner Mongolia, NE China: Insight into the source of brGDGTs. Org. Geochem. 112, 127–136.
Li, J., Pancost, R.D., Naafs, B.D.A., Yang, H., Liu, D., Gong, L., Qiu, X., Xie, S., 2019. Multiple environmental and ecological controls on archaeal ether lipid distributions in saline ponds. Chem. Geol. 529, 119293.
Liu, C., Zhu, L., Wang, J., Ju, J., Ma, Q., Qiao, B., Wang, Y., Xu, T., Chen, H., Kou, Q., Zhang, R., Kai, J., 2021. In-situ water quality investigation of the lakes on the Tibetan Plateau. Sci. Bull. 66 (17), 1727–1730.
Loomis, S.E., Russell, J.M., Ladd, B., Street-Perrott, F.A., Sinninghe Damsté, J.S., 2012. Calibration and application of the branched GDGT temperature proxy on East African lake sediments. Earth Planet. Sc Lett. 357-358, 277–288.
Macalady, J.L., Vestling, M.M., Baumler, D., Boekelheide, N., Kaspar, C.W., Banfield, J. F., 2004. Tetraether-linked membrane monolayers in Ferroplasma spp: a key to survival in acid. Extremophiles. 8 (5), 411–419.
Martin, C., Menot, G., Thouveny, N., Davtian, N., Andrieu-Ponel, V., Reille, M., Bard, E., 2019. Impact of human activities and vegetation changes on the tetraether sources in Lake St Front (Massif Central, France). Org. Geochem. 135, 38–52.
Martínez-Sosa, P., Tierney, J.E., 2019. Lacustrine brGDGT response to microcosm and mesocosm incubations. Org. Geochem. 127, 12–22.
Martínez-Sosa, P., Tierney, J.E., Meredith, L.K., 2020. Controlled lacustrine microcosms show a brGDGT response to environmental perturbations. Org. Geochem. 145, 104041.
Martínez-Sosa, P., Tierney, J.E., Stefanescu, I.C., Crampton-Flood, E.D., Shuman, B.N., Routson, C., 2021. A global Bayesian temperature calibration for lacustrine brGDGTs. Geochim. Cosmochim. Acta 305, 87–105.
Miller, D.R., Habicht, M.H., Keisling, B.A., Castañeda, I.S., Bradley, R.S., 2018. A 900-year New England temperature reconstruction from in situ seasonally produced branched glycerol dialkyl glycerol tetraethers (brGDGTs). Clim. Past 14 (11), 1653–1667.
Muller, G., Forstner, U., Irion, G., 1972. Formation and diagenesis of inorganic Ca-Mg carbonates in the lacustrine environment. Naturwissenschaften. 59 (4), 158–164.
Ning, D., Zhang, E., Shulmeister, J., Chang, J., Sun, W., Ni, Z., 2019. Holocene mean annual air temperature (MAAT) reconstruction based on branched glycerol dialkyl glycerol tetraethers from Lake Ximenglongtan, southwestern China. Org. Geochem. 133, 65–76.
Pancost, R.D., McClymont, E.L., Bingham, E.M., Roberts, Z., Charman, D.J., Hornibrook, E.R.C., Blundell, A., Chambers, F.M., Lim, K.L.H., Evershed, R.P., 2011. Archaeol as a methanogen biomarker in ombrotrophic bogs. Org. Geochem. 42 (10), 1279–1287.
Pearson, A., Ingalls, A.E., 2013. Assessing the use of archaeal lipids as marine environmental proxies. Annu. Rev. Earth Pl. Sc. 41 (1), 359–384.
Pearson, E.J., Juggins, S., Talbot, H.M., Weckstrom, J., Rosen, P., Ryves, D.B., Roberts, S. J., Schmidt, R., 2011. A lacustrine GDGT-temperature calibration from the Scandinavian Arctic to Antarctic: renewed potential for the application of GDGT-paleothermometry in lakes. Geochim. Cosmochim. Acta 75 (20), 6225–6238.
Pei, H., Wang, C., Wang, Y., Yang, H., Xie, S., 2019. Distribution of microbial lipids at an acid mine drainage site in China: Insights into microbial adaptation to extremely low pH conditions. Org. Geochem. 134, 77–79.
Pei, H., Zhao, S., Yang, H., Xie, S., 2021. Variation of branched tetraethers with soil depth in relation to non-temperature factors: Implications for paleoclimate reconstruction. Chem. Geol. 572.
Qian, S., Yang, H., Dong, C., Wang, Y., Wu, J., Pei, H., Dang, X., Lu, J., Zhao, S., Xie, S., 2019. Rapid response of fossil tetraether lipids in lake sediments to seasonal environmental variables in a shallow lake in Central China: Implications for the use of tetraether-based proxies. Org. Geochem. 128, 108–121.
Russell, J.M., Hopmans, E.C., Loomis, S.E., Liang, J., Sinninghe Damsté, J.S., 2018. Distributions of 5- and 6-methyl branched glycerol dialkyl glycerol tetraethers (brGDGTs) in East African lake sediment: Effects of temperature, pH, and new lacustrine paleotemperature calibrations. Org. Geochem. 117, 56–69.
Schouten, S., Hopmans, E.C., Sinninghe Damsté, J.S., 2013. The Org. Geochem. Of glycerol dialkyl glycerol tetraether lipids: a review. Org. Geochem. 54, 19–61.
Siliakus, M.F., van der Oost, J., Kengen, S.W.M., 2017. Adaptations of archaeal and bacterial membranes to variations in temperature, pH and pressure. Extremophiles. 21 (4), 651–670.
Sinninghe Damsté, J.S., Hopmans, E.C., Pancost, R.D., Schouten, S., Geenevasen, J.A.J., 2000. Newly discovered non-isoprenoid glycerol dialkyl glycerol tetraether lipids in sediments. Chem. Commun. 17, 1683–1684.
Smol, J.P., Cumming, B.F., 2000. Tracking long-term changes in climate using algal indicators in lake sediments. J. Phycol. 36 (6), 986–1011.
Stefanescu, I.C., Shuman, B.N., Tierney, J.E., 2021. Temperature and water depth effect on brGDGT distributions in sub-alpine lakes of mid-latitude North America. Org. Geochem. 152, 104174.
Sun, Q., Chu, G., Liu, M., Xie, M., Li, S., Ling, Y., Wang, X., Shi, L., Jia, G., Lu, H., 2011. Distributions and temperature dependence of branched glycerol dialkyl glycerol tetraethers in recent lacustrine sediments from China and Nepal. J. Geophys. Res. 116 (G1).
Tierney, J.E., Russell, J.M., 2009. Distributions of branched GDGTs in a tropical lake system: Implications for lacustrine application of the MBT/CBT paleoproxy. Org. Geochem. 40 (9), 1032–1036.
Tierney, J.E., Russell, J.M., Eggermont, H., Hopmans, E.C., Verschuren, D., Damste, J.S. S., 2010. Environmental controls on branched tetraether lipid distributions in tropical East African lake sediments. Geochim. Cosmochim. Acta 74 (17), 4902–4918.
Tierney, J.E., Schouten, S., Pitcher, A., Hopmans, E.C., Sinninghe Damsté, J.S., 2012. Core and intact polar glycerol dialkyl glycerol tetraethers (GDGTs) in Sand Pond, Warwick, Rhode Island (USA): Insights into the origin of lacustrine GDGTs. Geochim. Cosmochim. Acta 77, 561–581.
Turich, C., Freeman, K.H., 2011. Archaeal lipids record paleosalinity in hypersaline systems. Org. Geochem. 42 (9), 1147–1157.
Verschuren, D., Laird, K.R., Cumming, B.F., 2000. Rainfall and drought in equatorial East Africa during the past 1,100 years. Nature. 403 (6768), 410–414.
Wang, H., Liu, W., Zhang, C., Jiang, H., Dong, H., Lu, H., Wang, J., 2013. Assessing the ratio of archaeol to caldarchaeol as a salinity proxy in highland lakes on the northeastern Qinghai–Tibetan Plateau. Org. Geochem. 54, 69–77.
Wang, H., Dong, H., Zhang, C., Jiang, H., Liu, Z., Zhao, M., Liu, W., 2015. Deglacial and Holocene archaeal lipid-inferred paleohydrology and paleotemperature history of Lake Qinghai, northeastern Qinghai-Tibetan Plateau. Quat. Res. 83, 116–126.
Wang, H., Liu, W., He, Y., Zhou, A., Zhao, H., Liu, H., Cao, Y., Hu, J., Meng, B., Jiang, J., 2021. Salinity-controlled isomerization of lacustrine brGDGTs impacts the associated MBT5ME' terrestrial temperature index. Geochim. Cosmochim. Acta 305, 33–48.
Wang, J., Huang, L., Ju, J., Daut, G., Wang, Y., Ma, Q., Zhu, L., Haberzettl, T., Baade, J., Mausbacher, R., 2019. Spatial and temporal variations in water temperature in a high-altitude deep dimictic mountain lake (Nam Co), central Tibetan Plateau. J. Great Lakes Res. 45 (2), 212–223.
Wang, J., Huang, L., Ju, J., Daut, G., Ma, Q., Zhu, L., Haberzettl, T., Baade, J., Mausbacher, R., Hamilton, A., Graves, K., Olsthoorn, J., Laval, B.E., 2020. Seasonal stratification of a deep, high-altitude, dimictic lake: Nam Co. Tibetan Plateau. J. Hydrol. 584.
Wang, M., Hou, J., Lei, Y., 2014. Classification of Tibetan lakes based on variations in seasonal lake water temperature. Sci. Bull. 59 (34), 4847–4855.
Warren, J.K., 2010. Evaporites through time: Tectonic, climatic and eustatic controls in marine and nonmarine deposits. Earth-Sci. Rev. 98 (3–4), 217–268.
Weber, Y., De Jonge, C., Rijpstra, W.I.C., Hopmans, E.C., Stadnitskaia, A., Schubert, C.J., Lehmann, M.F., Damste, J.S.S., Niemann, H., 2015. Identification and carbon isotope composition of a novel branched GDGT isomer in lake sediments: evidence for lacustrine branched GDGT production. Geochim. Cosmochim. Acta 154, 118–129.
Weber, Y., Damste, J.S.S., Zopfi, J., De Jonge, C., Gilli, A., Schubert, C.J., Lepori, F., Lehmann, M.F., Niemann, H., 2018. Redox-dependent niche differentiation provides evidence for multiple bacterial sources of glycerol tetraether lipids in lakes. P. Natl. Acad. Sci. U.S.A. 115 (43), 10926–10931.
Weijers, J.W.H., Schouten, S., van den Donker, J.C., Hopmans, E.C., Sinninghe Damsté, J. S., 2007. Environmental controls on bacterial tetraether membrane lipid distribution in soils. Geochim. Cosmochim. Acta 71 (3), 703–713.
Weijers, J.W.H., Wiesenberg, G.L.B., Bol, R., Hopmans, E.C., Pancost, R.D., 2010. Carbon isotopic composition of branched tetraether membrane lipids in soils suggest a rapid turnover and a heterotrophic life style of their source organism(s). Biogeosciences 7, 2959–2973.
Wu, G., Liu, Y., He, B., Bao, Q., Duan, A., Jin, F., 2012. Thermal controls on the Asian summer monsoon. Sci. Rep. 2, 404.
Wu, J., Yang, H., Pancost, R.D., Naafs, B.D.A., Qian, S., Dang, X., Sun, H., Pei, H., Wang, R., Zhao, S., Xie, S., 2021. Variations in dissolved O_2 in a Chinese lake drive changes in microbial communities and impact sedimentary GDGT distributions. Chem. Geol. 579.
Xiao, W., Xu, Y., Ding, S., Wang, Y., Zhang, X., Yang, H., Wang, G., Hou, J., 2015. Global calibration of a novel, branched GDGT-based soil pH proxy. Org. Geochem. 89-90, 56–60.
Xiao, W., Wang, Y., Zhou, S., Hu, L., Yang, H., Xu, Y., 2016. Ubiquitous production of branched glycerol dialkyl glycerol tetraethers (brGDGTs) in global marine environments: a new source indicator for brGDGTs. Biogeosciences. 13 (20), 5883–5894.
Xiao, W., Wang, Y., Liu, Y., Zhang, X., Shi, L., Xu, Y., 2020. Predominance of hexamethylated 6-methyl branched glycerol dialkyl glycerol tetraethers in the Mariana Trench: source and environmental implication. Biogeosciences. 17 (7), 2135–2148.

Yang, H., Pancost, R.D., Dang, X., Zhou, X., Evershed, R.P., Xiao, G., Tang, C., Gao, L., Guo, Z., Xie, S., 2014. Correlations between microbial tetraether lipids and environmental variables in Chinese soils: Optimizing the paleo-reconstructions in semi-arid and arid regions. Geochim. Cosmochim. Acta 126, 49–69.

Yang, H., Lu, X., Ding, W., Lei, Y., Dang, X., Xie, S., 2015. The 6-methyl branched tetraethers significantly affect the performance of the methylation index (MBT′) in soils from an altitudinal transect at Mount Shennongjia. Org. Geochem. 82, 42–53.

Yang, J., Jiang, H., Dong, H., Liu, Y., 2019. A comprehensive census of lake microbial diversity on a global scale. Sci. China-Life Sci. 62 (10), 1320–1331.

Yao, Y., Zhao, J., Vachula, R.S., Werne, J.P., Wu, J., Song, X., Huang, Y., 2020. Correlation between the ratio of 5-methyl hexamethylated to pentamethylated branched GDGTs (HP5) and water depth reflects redox variations in stratified lakes. Org. Geochem. 147, 104076.

Zhang, E., Shen, J., Wang, S., Yin, Y., Zhu, Y., Xia, W., 2004. Quantitative reconstruction of the paleosalinity at Qinghai Lake in the past 900 years. Sci. Bull. 49 (7), 730–734.

Zhang, G., Yao, T., Xie, H., Yang, K., Zhu, L., Shum, C.K., Bolch, T., Yi, S., Allen, S., Jiang, L., Chen, W., Ke, C., 2020. Response of Tibetan Plateau lakes to climate change: Trends, patterns, and mechanisms. Earth-Sci. Rev. 208.